Monte Carlo calculations of the replacement correction factor, P_{repl}, for cylindrical chamber cavities in clinical photon and electron beams

Fujio Araki,[a)]

Department of Radiological Technology, Faculty of Life Sciences, Kumamoto University, 4-24-1, Kuhonji, Kumamoto, 862-0976, Japan

e-mail: f_araki@kumamoto-u.ac.jp

TEL/FAX: +81-96-373-5488

E-mail: f_araki@kumamoto-u.ac.jp

Abstract

The purpose of this study was to calculate the replacement correction factor, P_{repl} (the product $P_{gr}P_{fl}$ in the AAPM's notation, or the product $p_{cav}p_{dis}$ in the IAEA's notation), at a reference depth, d_{ref}, for cylindrical chamber cavities in clinical photon and electron beams by Monte Carlo simulation. P_{repl} was calculated for cavities with a combination of various diameters and lengths. P_{repl} values calculated in photon and electron beams were typically higher than those recommended by the TG-51 and TRS-398 dosimetry protocols. P_{repl} values for a Farmer chamber cavity were higher by 0.3% to 0.2% and by 0.7% to 0.4%, respectively, than data of TG-51 and TRS-398, at photon energies of ^{60}Co to 18 MV. Similarly, the P_{repl} values for electron beams were higher by 1.5% to 1.1% than data for both protocols, in a range of 6 MeV to 18 MeV. The P_{repl} values depended upon the cavity diameter and length, especially for lower electron energies. We found that P_{repl} values of cylindrical chamber cavities for photon and electron beams were significantly different from those recommended by TG-51 and TRS-398.

Key words: replacement correction factor, cylindrical ion chamber, clinical dosimetry protocols, Monte Carlo calculations

1 Introduction

In ion chamber dosimetry protocols [1-4], the replacement correction factor, P_{repl}, accounts for the medium of interest being replaced by the air cavity of the chamber. In the AAPM dosimetry protocol, $P_{repl}=P_{gr}P_{fl}$, where P_{gr} is the gradient correction and P_{fl} is the fluence correction (corresponding to the displacement perturbation, p_{dis}, and the fluence perturbation, p_{cav}, respectively, in the IAEA's notations). P_{gr} accounts for the shift upstream of the effective point of measurement of the chamber due to the air cavity. P_{fl} corrects for changes in the electron fluence spectrum due to the presence of the air cavity, predominantly the in-scattering of electrons that makes the electron fluence inside the cavity different from that in the medium in the absence of the cavity. It is conceptually difficult, if not impossible, rigorously to separate the two corrections because both are related to the effects of the cavity in the medium.

For cylindrical chambers in photon beams, P_{fl} is not required for dose determinations made at or beyond the depth of the maximum dose, d_{max}, where a transient electron equilibrium exists. P_{gr} in the AAPM TG-51 and the IAEA TRS-398 protocols is based on different sources. The TG-51 values are based on the work of Cunningham and Sontag [5], which is a mixture of measurements and mostly analytical calculations. For TRS-398, the values are nominally based on the measured data of Johansson *et al*. [6]. The values for the correction factor given by TG-51 are higher than the data of Johansson *et al*. by up to 0.6% for a Farmer-type chamber, and even more for chambers of larger diameter. It is clear that P_{gr} represents a significant uncertainty in the present dosimetry protocols. The uncertainty of the P_{gr} ratio entering into the beam quality conversion factor, k_Q, is estimated at 0.5% in TRS-398. However, in practice, the differences of P_{gr} values in both protocols have a reduced effect because only the ratios are used.

In electron beams, both protocols recommend the effective point of measurement which approaches to correct for the gradient (P_{gr}), that is, the method treats the point of measurement as being $0.5r$ upstream of the center of the chamber cavity, where r is the radius of the chamber cavity. For the TRS-398 P_{fl} values, the experimental data of Johansson *et al*. [6] have been recast in terms of the radius of the chamber cavity and the beam quality R_{50}, and they were fitted with the approximate equation. TRS-398

recommends the use of cylindrical chambers for beam qualities just above R_{50}=4 cm. Similarly, The TG-51 P_{fl} values are derived from AAPM TG-21 [7] based on the experimental data of Johansson *et al*. [6]. The cylindrical chambers may be used for beam qualities with $R_{50} \geq 2.6$ cm only and preferably $R_{50} \geq 4.3$ cm. The P_{fl} values of cylindrical chambers for $R_{50} \geq 4$ cm are almost the same in both protocols. The correction for most chamber types is less than 0.3%, and the uncertainty is estimated to be 0.5% in TRS-398.

Recently, Wang and Rogers [8,9] have calculated P_{repl} for photon and electron beams by using the EGSnrc C++-based user-code Cavity [10,11]. For a Farmer chamber cavity, the P_{repl} value in a ^{60}Co beam is 0.4% higher and 0.8% higher, respectively, than those recommended by TG-51 and TRS-398. Wang and Rogers [8,9] indicate that the discrepancy is likely to be due to a misinterpretation of the calculations and measurements by Cunningham and Sontag [5] as used by TG-51 (or TG-21), and of the experimental measurements by Johansson *et al*. [6] adopted in TRS-398. Similarly, the calculated P_{repl} values for a Farmer chamber cavity in electron beams are also higher by up to 1% compared to both protocols. Wang and Rogers [8,9] explain this as follows: the discrepancy exists because the experimental data of Johansson *et al*. [6] adopted in both protocols are based on the assumption that the wall correction factor P_{wall} and P_{repl} at a reference depth, d_{ref}, for the plane-parallel chamber used in the comparison with the Farmer chamber are unity. Recent studies [12-14] show that the product of P_{wall} and P_{repl} for the plane-parallel chamber is higher than unity by up to approximately 1%.

In this study, we calculated P_{repl} at d_{ref} for the cylindrical chamber cavities in clinical photon and electron beams by using the EGSnrc C++-based user-code Cavity. The chamber cavities were used in a combination of various diameters and lengths to simulate real chambers. The P_{repl} values were compared with data recommended by TG-51 and TRS-398, and with recently published data [8,9]. The chamber size dependence and the beam quality dependence of P_{repl} values were also analyzed in detail.

2 Methods

2.1 Calculation methods

In ion chamber dosimetry, the dose to water, D_w, is related to the dose to the air cavity, D_{air}, of

a chamber with the point of measurement at the same location in water according to the Spencer-Attix cavity theory:

$$\frac{D_w}{D_{air}} = \left(\frac{\bar{L}}{\rho}\right)^w_{air} P_{repl} P_{wall} P_{cel}, \qquad (1)$$

where $(\bar{L}/\rho)^w_{air}$ is the average restricted mass collision stopping-power ratio (SPR) of water to air, P_{wall} corrects for the chamber wall material being different from the medium, and P_{cel} corrects for the central electrode being different from the cavity medium. For a water-walled chamber with no central electrode,

$$\frac{D_w}{D_{air}} = \left(\frac{\bar{L}}{\rho}\right)^w_{air} P_{repl}. \qquad (2)$$

Equation (2) represents an indirect method of calculating P_{repl} by using SPR. In this study, we computed P_{repl} with a direct method by using a "low density water" (LDW) material [15-18]. The LDW method replaces the air cavity for cylindrical chambers with the LDW material. LDW is an artificial material that has all the dosimetric properties of nominal water except that its density is equal to that of air. The LDW method avoids SPR in the calculation of P_{repl}. P_{repl} is thus calculated directly as the ratio of the dose to water and the dose to the LDW cavity for cylindrical chambers at d_{ref} in a water phantom,

$$P_{repl} = \frac{D_w}{D_{LDW}}. \qquad (3)$$

2.2 Monte Carlo calculations of P_{repl}

The P_{repl} values at d_{ref} for cylindrical chamber cavities were calculated for a ^{60}Co beam and 4, 6, 10, 15, and 18 MV x-ray beams, as well as 6, 9, 12, 15, and 18 MeV electron beams. Table 1 presents the characteristics of photon and electron beams from the Varian Clinac linear accelerators (Varian Oncology Systems, Palo Alto, CA) used in this study. Also shown is the beam quality for a ^{60}Co beam. The doses to water and the LDW cavity in a water phantom were computed with the EGSnrc C++-based user-code Cavity. The radiation source was at 80 cm source-surface distance (SSD) for a ^{60}Co beam and at 100 cm SSD for x-ray beams, with a field size of 10×10 cm^2, and at 100 cm SSD for electron beams with a field size of 15×15 cm^2. The spectrum for the ^{60}Co calculations was obtained from Mora *et al*.[19] The spectra of the incident x-ray and electron beams were calculated from the EGSnrc [20]/BEAMnrc [21,22] simulation for the Varian machines mentioned above. The water phantom was a cube with 30

cm sides. The dose to water was computed for a slab with a radius of 1 cm and a thickness of 0.1 mm in the water phantom. The point of measurement for the LDW-filled cavity was taken to be its geometric center and was located at depths of 5 cm and 10 cm for the ^{60}Co beam and x-ray beams, respectively. For electron beams, the point of measurement was at 0.5r (r is the radius of the chamber cavity) deeper than the reference depth. The sizes of the LDW cavities in this study were used in a combination of diameters from 8 mm to 2 mm and lengths of 20 mm, 10 mm, and 5 mm to simulate real chambers available commercially.

P_{repl} for electron beams in this study was calculated with the center of the chamber cavity positioned at depth d_{ref}+0.5r according to TRS-398, as follows:

$$P_{repl}^{LDW}(d_{ref}+0.5r)=\frac{D_w(d_{ref})}{D_{LDW}(d_{ref}+0.5r)}. \qquad (4)$$

P_{repl} corresponds to p_{cav} (P_{fl} in the AAPM's notation) in TRS-398, but it is difficult to separate them strictly due to the uncertainty of p_{dis} (P_{gr} in the AAPM's notation). Here, it should be noted that $P_{repl}^{LDW}(d_{ref}+0.5r)$ is related to the dose in the water phantom, $D_w(d_{ref})$, at d_{ref}.

The doses to water and LDW materials were computed with a statistical uncertainty (1σ) of 0.1%. The energy threshold and cutoff for the Cavity code were set to AE=ECUT=0.521 MeV and AP=PCUT=0.01 MeV, respectively. The P_{repl} values calculated at d_{ref} for photon and electron beams were compared with data recommended by the TG-51 and TRS-398 dosimetry protocols, and with recently published data [8,9]. The cavity size dependence and the beam quality dependence of P_{repl} were also analyzed for combinations of various cavity diameters and lengths.

3 Results and discussion

3.1 P_{repl} for photon beams

Figures 1(a), 1(b), and 1(c) show a comparison of P_{repl} values at d_{ref} for various cavity diameters as a function of a beam quality specifier, $TPR_{20,10}$, and for the lengths of 20 mm, 10 mm, and 5 mm, respectively. The radiation source for a ^{60}Co beam was calculated at 80 cm SSD and a depth of 5 cm, which differs from the geometry for x-ray beams. All of the P_{repl} values varied from 0.994 to 0.998 for cylindrical cavities with diameters from 8 mm to

2 mm that are available commercially. The P_{repl} values approached unity as the cavity diameter became smaller. The P_{repl} values for each cavity diameter were almost independent of the beam quality and were in agreement within approximately 0.2%. As for the Farmer chamber cavity (wall-less, without central electrode) with a diameter of 6 mm and a length of 20 mm, the P_{repl} values were 0.9951-0.9968 in the range of ^{60}Co to 18 MV, and they agreed within 0.1% with those of Wang and Rogers [8]. Their value for ^{60}Co was 0.9961, which was calculated at 100 cm SSD and a depth of 10 cm. As a result, the $P_{repl,Q}/P_{repl,Co}$ ratio of beam quality Q to ^{60}Co included in the k_Q factor was close to unity.

Figures 2(a), 2(b), and 2(c) show a comparison of P_{repl} values at d_{ref} for different cavity lengths as a function of $TPR_{20,10}$ and for diameters of 6 mm, 4 mm, and 3 mm, respectively. The values of TG-51 and TRS-398 are also presented in Fig. 2. A slight cavity length dependence of the P_{repl} values for each cavity diameter is shown, but the differences were still within 0.2%. The P_{repl} values tend to be lower as the cavity length becomes shorter. This is because the electron fluence per unit volume entering the cavity from the water phantom increases relatively. P_{repl} of the Farmer chamber cavity was higher by 0.3% to 0.2% and by 0.7% to 0.4%, respectively, than the data of TG-51 and TRS-398, in the range of ^{60}Co to 18 MV. The differences decreased as the cavity diameter became smaller. The calculated $P_{repl,Q}/P_{repl,Co}$ ratios for cylindrical chamber cavities were almost independent of the beam quality, unlike those in TG-51 and TRS-398.

Figures 3(a) to 3(f) show a comparison of P_{repl} values at d_{ref} as a function of cavity diameters for the lengths of 20 mm, 10 mm, and 5 mm and for photon energies of ^{60}Co to 18 MV. The P_{repl} values approached unity as the cavity diameter became smaller and its length greater. The variation of P_{repl} for the cavity diameters and lengths is almost independent of the beam quality. The magnitude in the P_{repl} variation was within approximately 0.3% for the cylindrical cavities with a combination of diameters from 8 mm to 2 mm and lengths from 20 mm to 5 mm that are available commercially.

3.2 P_{repl} for electron beams

Figures 4(a), 4(b), and 4(c) show a comparison of calculated P_{repl} values at d_{ref} for various cavity diameters as a function of R_{50} and for lengths of 20 mm, 10 mm, and 5 mm,

respectively. The P_{repl} values were strongly dependent on the cavity diameter and electron energy, unlike the case of photon beams, and approached unity as the cavity diameter became smaller and the electron energy increased. For the Farmer chamber cavity, P_{repl} values varied from 0.973 to 0.989 in the range of 6 MeV to 18 MeV (R_{50}=2.37 cm to 7.60 cm).

Figures 5(a) to 5(d) show a comparison of P_{repl} values at d_{ref} for different cavity lengths as a function of R_{50} and for diameters from 6 mm to 3 mm. The values of TG-51 and TRS-398 are also presented in Fig. 5. P_{repl} for TRS-398 is shown at $R_{50} \geq 4$ cm and was in good agreement within 0.1% with that of TG-51. The P_{repl} values were typically higher than those of TG-51 and TRS-398, which are based on the experimental data of Johansson *et al*. [6]. For the Farmer chamber cavity, calculated P_{repl} values were higher by 1.5% to 1.1% than the TG-51 data, in the range of 6 MeV to 18 MeV. The differences are close to the product of perturbation factors, $P_{wall}P_{repl}$ [12-14], at d_{ref} for the well-guarded plane-parallel chambers used in the comparison with the Farmer chamber as described by Wang and Rogers [9]. The P_{repl} value for the cavity diameter of 6 mm and the length of 5 mm was 0.8% lower than that of the length of 20 mm at 6 MeV. The cavity length dependence of P_{repl} decreased as the cavity diameter became smaller and the electron energy increased. P_{repl} for the cavity diameter of 3 mm was almost independent of the cavity length.

Figures 6(a) to 6(e) show a comparison of P_{repl} values at d_{ref} as a function of cavity diameters for the lengths of 20 mm, 10 mm, and 5 mm and for electron energies from 6 MeV to 18 MeV. It can be seen that the P_{repl} values depended strongly on the cavity diameter and length and on the electron energy. The effect of the cavity length for P_{repl} was insignificant for higher-energy electrons of 18 MeV.

P_{repl} calculated at d_{ref} in the range from 6 MeV to 18 MeV is compared with that of Wang and Rogers [9] in Fig. 7, which is symbolized as P_{fl} in their paper. The P_{repl} values for cylindrical chamber cavities with diameters of 8 mm, 6 mm, and 4 mm and a length of 20 mm agreed within 0.2% with their data, except at 6 MeV. The P_{repl} values of Wang and Rogers [9] were calculated with the center of the chamber cavity positioned at depth d_{ref} according to TG-51. In contrast, P_{repl} in this study was calculated with the cavity center

located at depth d_{ref}+0.5r by Eq. (4) according to TRS-398. The differences between P_{repl} values at the two depths for 6 MeV were 1.6% and 0.7%, respectively, for the cavity diameters of 8 mm and 6 mm, and 0.1% for the 4 mm diameter. The results support the TG-51 and TRS-398 protocols which recommend a beam quality $R_{50} \geq 4$ cm for use of a Farmer chamber in electron beam calibration.

4 Conclusions

P_{repl} at d_{ref} for cylindrical chamber cavities with various diameters and lengths have been calculated for clinical photon and electron beams by EGSnrc Monte Carlo simulation. P_{repl} values for a Farmer chamber cavity were higher by 0.3% to 0.2% and by 0.7% to 0.4%, respectively, than data of TG-51 and TRS-398, at photon energies of ^{60}Co to 18 MV. The cavity length dependence of P_{repl} for cavity diameters from 6 mm to 3 mm was within 0.2%. The $P_{repl,Q}/P_{rpel,Co}$ ratios for the cylindrical cavities were almost independent of the photon beam quality. The P_{repl} values of a Farmer chamber cavity for electron beams were higher by 1.5% to 1.1% than data of TG-51 and TRS-398, in the range of 6 MeV to 18 MeV. The P_{repl} values depended upon the cavity diameter and length, especially for lower electron energies. We found that P_{repl} values for cylindrical chamber cavities in photon and electron beams were significantly different from those recommended by TG-51 and TRS-398.

References

1. Almond PR, Biggs PJ, Coursey BM, Hanson WF, Huq MS, Nath R, and Rogers DWO. AAPM's TG-51 protocol for clinical reference dosimetry of high-energy photon and electron beams. Med Phys. 1999;26:1847-70.
2. IAEA. Absorbed dose determination in external beam radiotherapy: An international code of practice for dosimetry based on standards for absorbed dose to water. Technical Report Series No. 398. IAEA, Vienna 2000.
3. JSMP: Japanese Society of Medical Physics. The standard dosimetry of absorbed dose in external beam radiotherapy. Tsusho-sangyo-kenkyusya, Tokyo, 2002 (in Japanese).
4. IPEM. The IPEM code of practice for electron dosimetry for radiotherapy beams of initial energy from 4 to 25 MeV based on an absorbed dose to water calibration. Phys Med Biol. 2003;48:2929-70.
5. Cunningham JR and Sontag MR. Displacement corrections used in absorbed dose

determinations. Med Phys. 1980;7:672-6.

6. Johansson KA, Mattsson LO, Lindborg L, and Svensson H. Absorbed-dose determination with ionization chambers in electron and photon beams having energies between 1 and 50 MeV. IAEA Symposium Proceeding, Vienna, 1977, p. 243-70.

7. AAPM TG-21. A protocol for the determination of absorbed dose from high-energy photon and electron beams. Med Phys. 1983;10:741-71.

8. Wang LLW and Rogers DWO, The replacement correction factors for cylindrical chambers in high-energy photon beams. Phys Med Biol. 2009;54:1609-20.

9. Wang LLW and Rogers DWO. Replacement correction factors for cylindrical ion chambers in electron beams. Med Phys. 2009;36:4600-8.

10. Kawrakow I, Mainegra-Hing E, Tessier F, and Walters BRB. The EGSnrc C++ class library. National Research Council of Canada Technical Report No. PIRS-898 (rev A), 2009. (unpublished) (http://www.irs.inms.nrc.ca/inms/irs/EGSnrc/PIRS898/)

11. Kawrakow I. egspp: the EGSnrc C++ class library. National Research Council of Canada Technical Report No. PIRS-899, 2005.

12. Buckley LA and Rogers DWO. Wall correction factors, P_{wall}, for parallel-plate ionization chambers. Med Phys. 2006;33:1788-96.

13. Zink K and Wulff J. Monte Carlo calculations of beam quality correction factors k_Q for electron dosimetry with a parallel-plate Roos chamber. Phys Med Biol. 2008;53:1595-607.

14. Araki F. Monte Carlo calculations of correction factors for plane-parallel ionization chambers in clinical electron dosimetry. Med Phys. 2008;35:4033-40.

15. Wang LLW and Rogers DWO. Calculation of the replacement correction factors for ion chambers in megavoltage beams by Monte Carlo simulation. Med Phys.2008;35:1747-55.

16. Wang LLW, La Russa DJ, and Rogers DWO. Systematic uncertainties in the Monte Carlo of ion chamber replacement correction factors. Med Phys. 2009;36:1785-9.

17. Kawrakow I. On the effective point of measurement in megavoltage photon beams, Med Phys.2006;33:1829-39.

18. Sempau J and Andreo P. Configuration of the electron transport algorithm of PENELOPE to simulate ion chambers. Phys Med Biol. 2006;51:3533-48.

19. Mora G, Maito A, and Rogers DWO. Monte Carlo simulation of a typical ^{60}Co therapy source. Med Phys. 1999;26:2494-502.

20. Kawrakow I, Mainegra-Hing E, Rogers DWO, Tessier F, and Walters BRB. The EGSnrc code system: Monte Carlo Simulation of Electron and Photon Transport. National Research Council of Canada Report PIRS-701, 2009.

21. Rogers DWO, Faddegon BA, Ding GX, Ma CM, We J, and Mackie TR. BEAM: a Monte Carlo code to simulate radiotherapy treatment units. Med Phys. 1995;22:503-24.

22. Rogers DWO, Walters BRB, and Kawrakow I. BEAMnrc Users Manual. National Research Council of Canada Report PIRS-509 (A) Rev K 2009.

Figure captions

Fig. 1. Comparison of P_{repl} values at d_{ref} for various cavity diameters as a function of $TPR_{20,10}$ and for lengths of (a) 20 mm, (b) 10 mm, and (c) 5 mm. The cavity dimensions were selected to simulate a real chamber.

Fig. 2. Comparison of P_{repl} values at d_{ref} for different cavity lengths as a function of $TPR_{20,10}$ and for diameters of (a) 6 mm, (b) 4 mm, and (b) 3 mm. The dashed lines show P_{repl} values of TG-51 and TRS-398.

Fig. 3. Comparison of P_{repl} values at d_{ref} as a function of cavity diameters for lengths of 20 mm, 10 mm, and 5 mm and for photon energies of (a) ^{60}Co, (b) 4 MV, (c) 6 MV, (d) 10 MV, (e) 15 MV, and (f) 18 MV.

Fig. 4. Comparison of P_{repl} values at d_{ref} for various cavity diameters as a function of R_{50} and for lengths of (a) 20 mm, (b) 10 mm, and (c) 5 mm. The cavity dimensions were selected to simulate a real chamber.

Fig. 5. Comparison of P_{repl} values at d_{ref} for differences in cavity lengths as a function of R_{50} and for diameters of (a) 6 mm, (b) 5 mm, (c) 4 mm, and (d) 3 mm. The dashed lines show P_{repl} values of TG-51 and TRS-398.

Fig. 6. Comparison of P_{repl} values at d_{ref} as a function of cavity diameters for lengths of 20 mm, 10 mm, and 5 mm and for electron energies of (a) 6 MeV, (b) 9 MeV, (c) 12 MeV, (d) 15 MeV, and (e) 18 MeV.

Fig. 7. Comparison of P_{repl} at d_{ref} calculated in this study (solid lines) and by Wang and Rogers (Ref. 9) (dashed lines) as a function of R_{50}. The cylindrical chamber cavities had diameters of 8 mm, 6 mm, and 4 mm with 20 mm length.

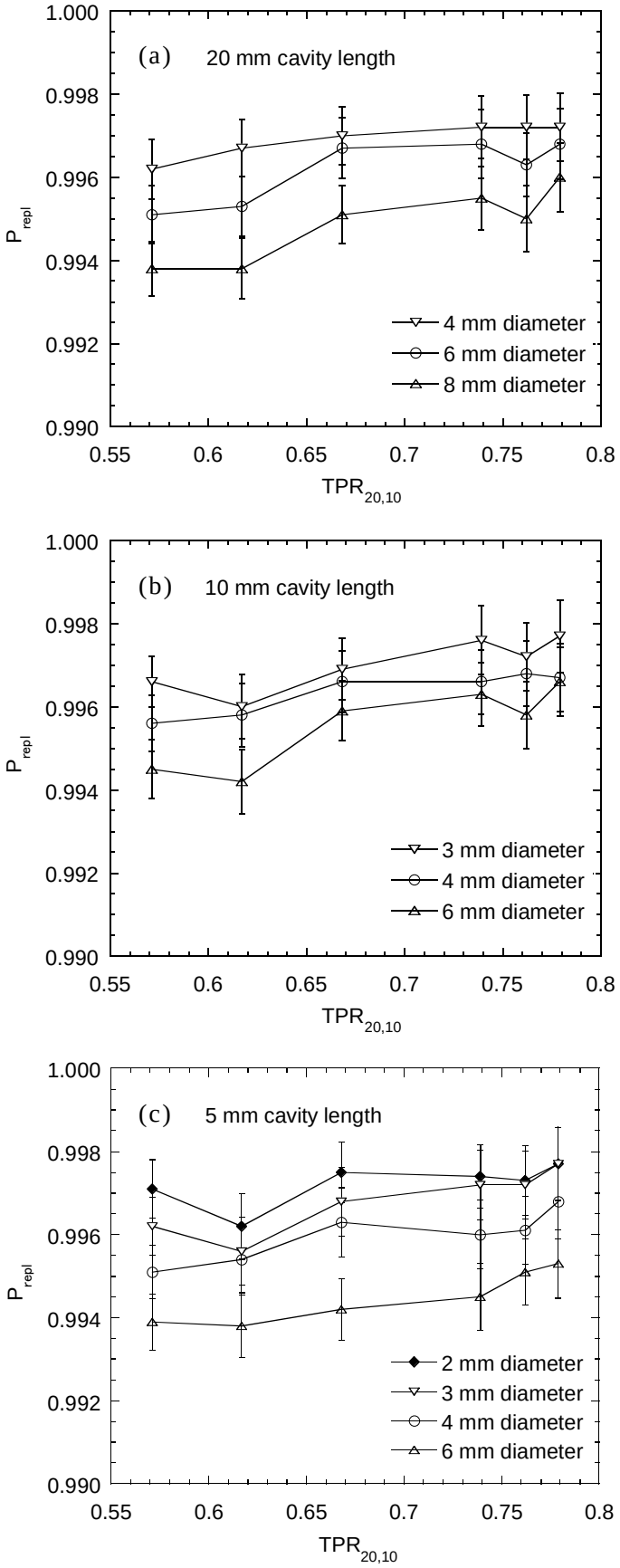

Fig. 1. Comparison of P_{repl} values at d_{ref} for various cavity diameters as a function of $\mathrm{TPR}_{20,10}$ and for lengths of (a) 20 mm, (b) 10 mm, and (c) 5 mm. The

cavity dimensions were selected to simulate a real chamber.

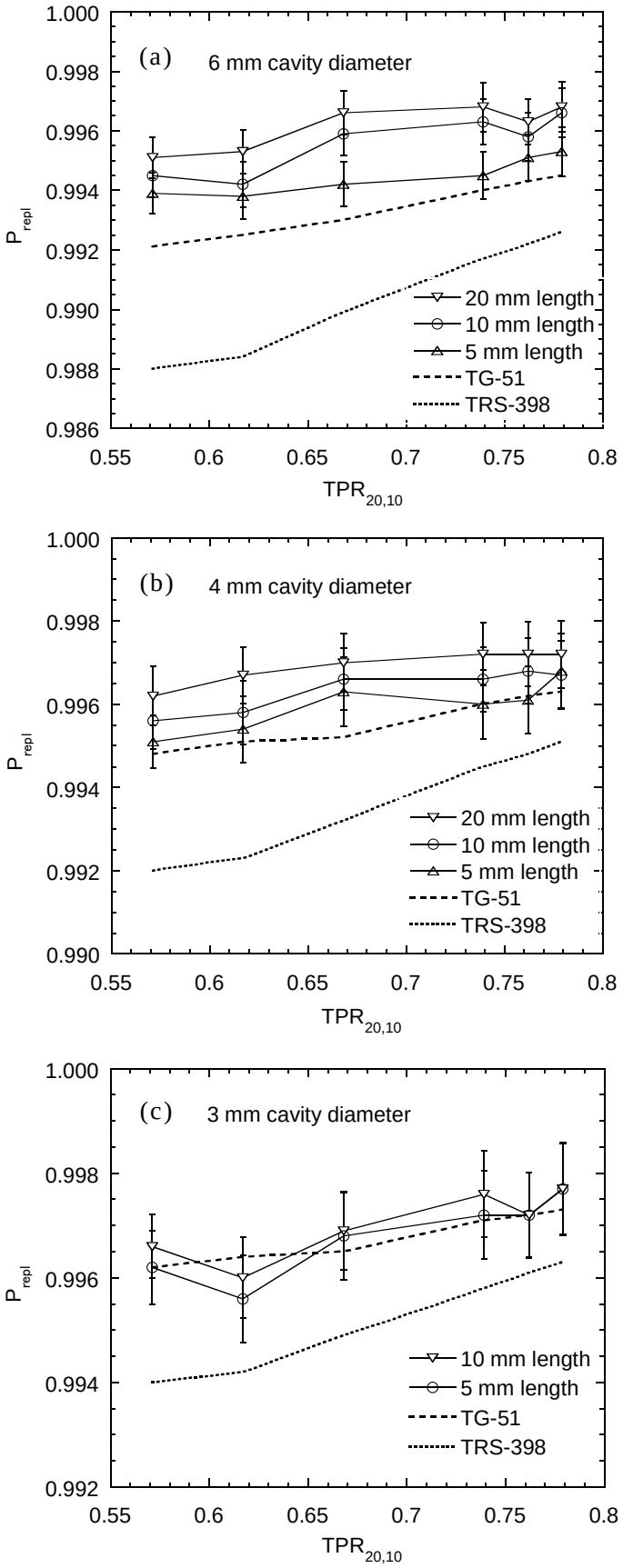

Fig. 2. Comparison of P_{repl} values at d_{ref} for different cavity lengths as a function of $\mathrm{TPR}_{20,10}$ and for diameters of (a) 6 mm, (b) 4 mm, and (c) 3 mm. The dashed lines

show P_{repl} values of TG-51 and TRS-398.

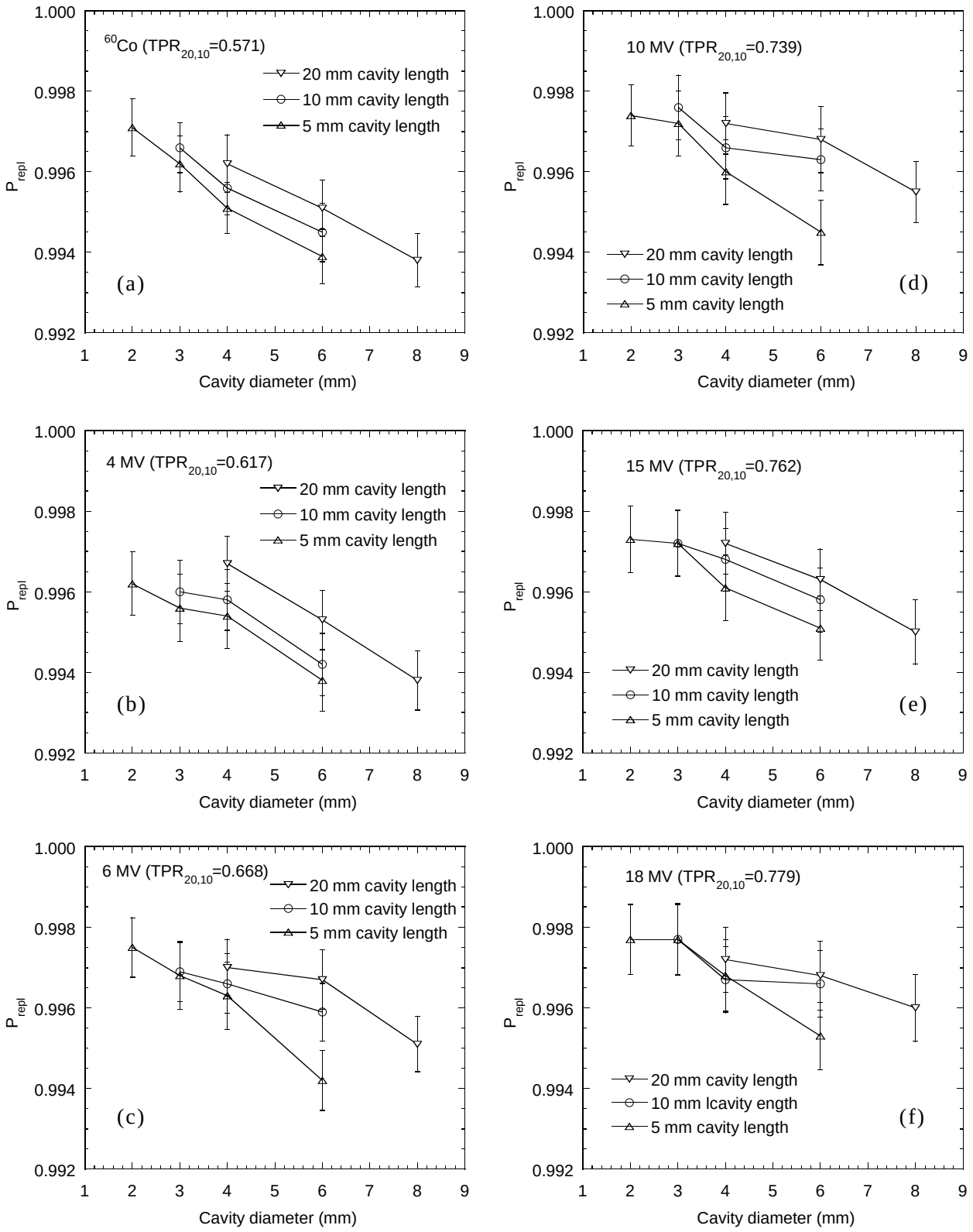

Fig. 3. Comparison of P_{repl} values at d_{ref} as a function of cavity diameters for lengths of 20 mm, 10 mm, and 5 mm and for photon energies of (a) ^{60}Co, (b) 4 MV, (c) 6 MV, (d) 10 MV, (e) 15 MV, and (f) 18 MV.

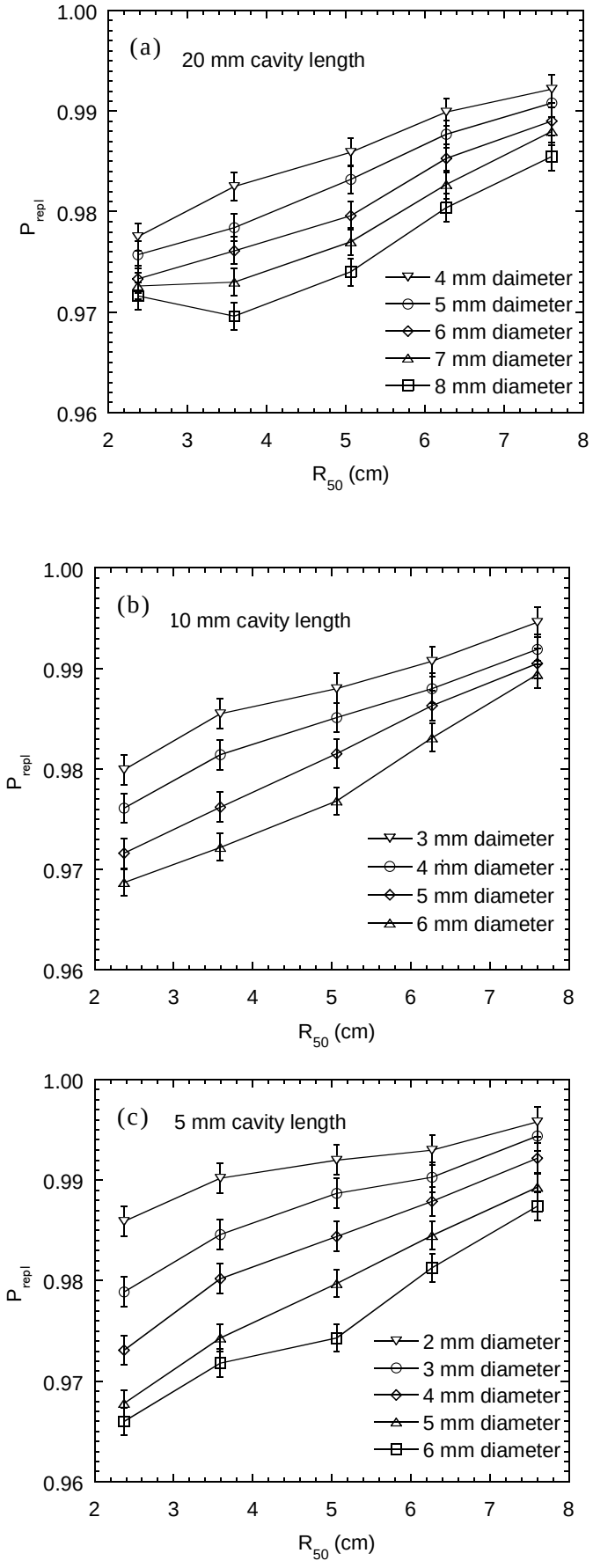

Fig. 4. Comparison of P_{repl} values at d_{ref} for various cavity diameters as a

function of R_{50} and for lengths of (a) 20 mm, (b) 10 mm, and (c) 5 mm. The cavity dimensions were selected to simulate a real chamber.

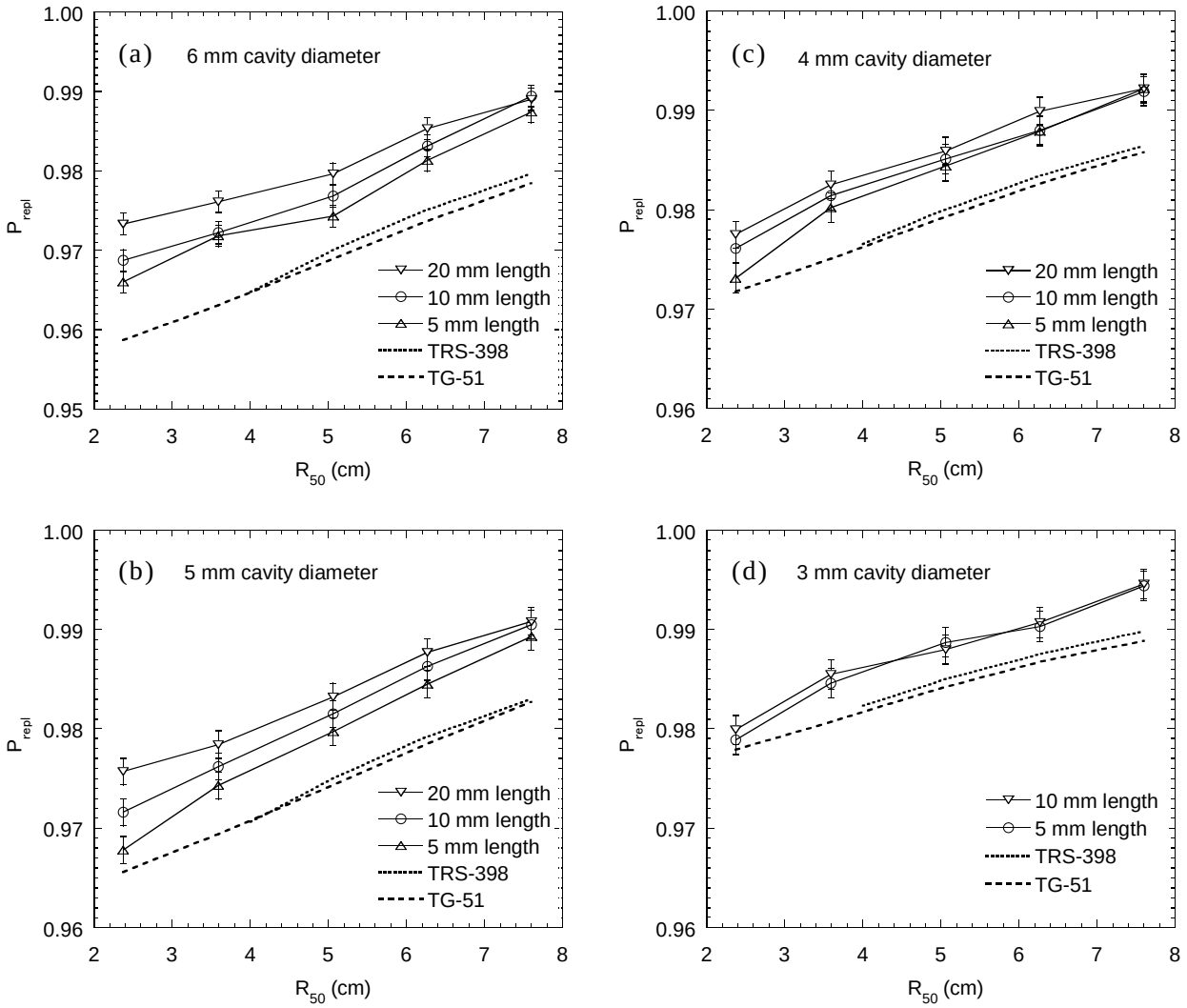

Fig. 5. Comparison of P_{repl} values at d_{ref} for differences in cavity lengths as a function of R_{50} and for diameters of (a) 6 mm, (b) 5 mm, (c) 4 mm, and (d) 3 mm. The dashed lines show P_{repl} values of TG-51 and TRS-398.

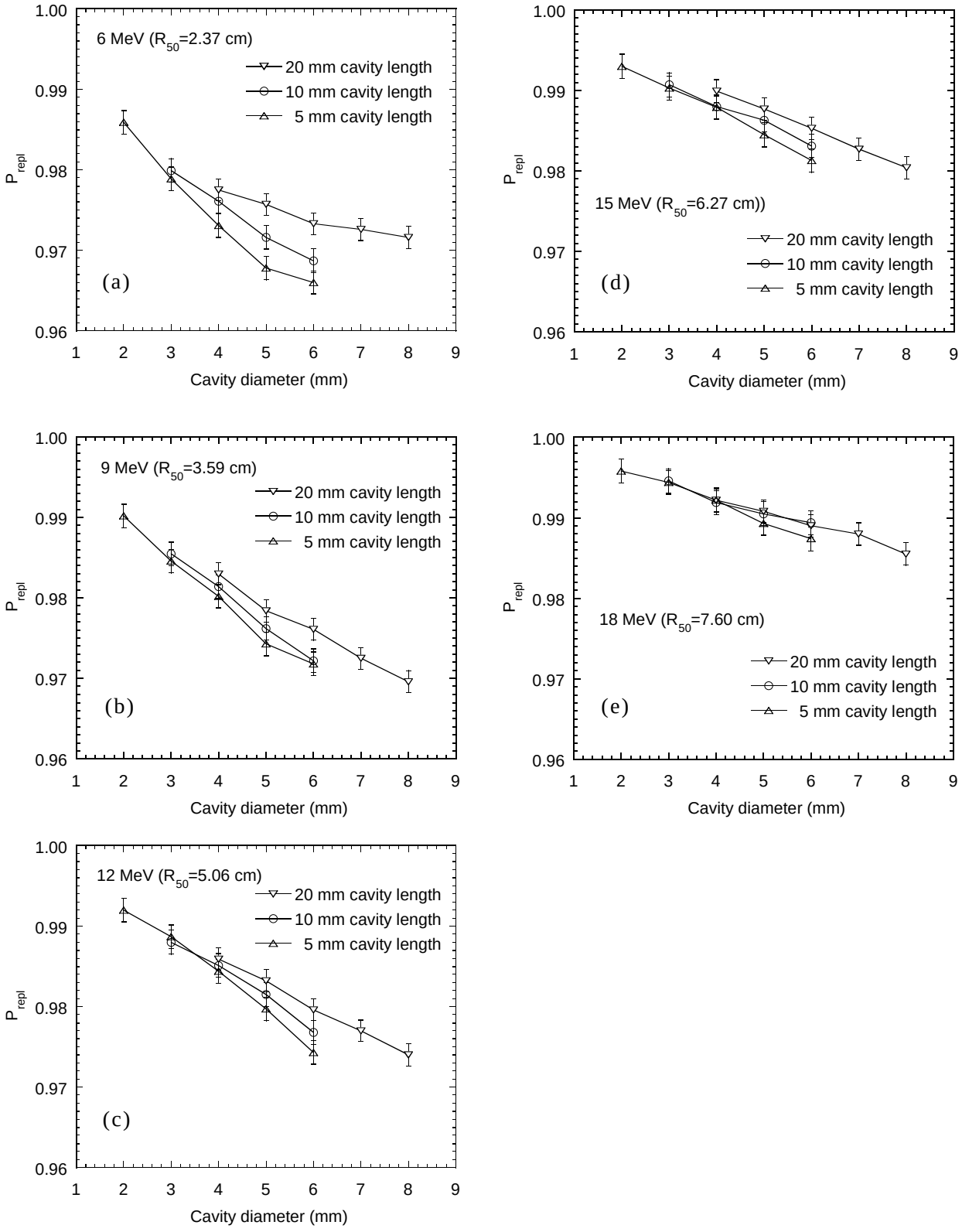

Fig. 6. Comparison of P_{repl} values at d_{ref} as a function of cavity diameters for lengths of 20 mm, 10 mm, and 5 mm and for electron energies of (a) 6 MeV, (b) 9 MeV, (c) 12 MeV, (d) 15 MeV, and (e) 18 MeV.

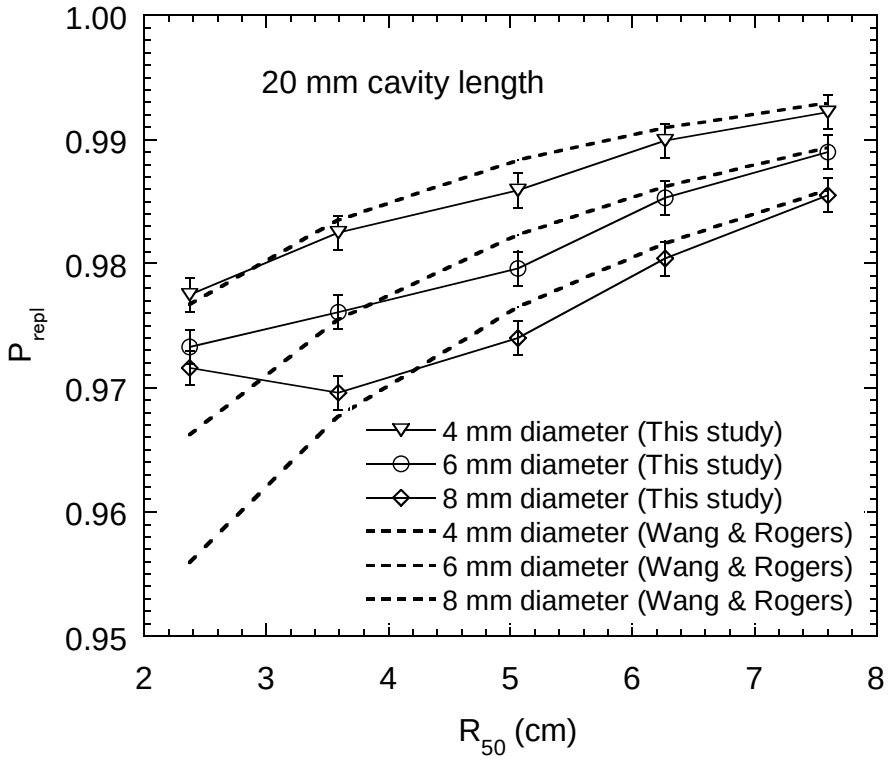

Fig. 7. Comparison of P_{repl} at d_{ref} calculated in this study (solid lines) and by Wang and Rogers (Ref. 9) (dashed lines) as a function of R_{50}. The cylindrical chamber cavities had diameters of 8 mm, 6 mm, and 4 mm with 20 mm length.

Table 1. Characteristics of photon and electron beams from the Varian Clinac linear accelerators used in this study. Also shown is the beam quality for a ^{60}Co beam.

Photon beams		
E_{nominal} (MV)	%dd(10)$_x$	TPR$_{20,10}$
^{60}Co	58.3	0.571
4	62.0	0.617
6	66.1	0.668
10	73.6	0.739
15	77.2	0.762
18	80.9	0.779
Electron beams		
E_{nominal} (MeV)	R_{50} (cm)	d_{ref} (cm)
6	2.37	1.32
9	3.59	2.05
12	5.06	2.94
15	6.27	3.66
18	7.60	4.46